Pharmaceutical Sciences Asia

Pharm Sci Asia 2024; 51(1), 59-73

DOI:10.29090/psa.2024.01.23.1061

Research Article

Exploring novel indomethacin-derived compounds via investigation of NSAIDs through molecular docking and *in vitro* testing for anti-amyloid beta aggregation

Somjate Laivut[1], Salinthip Jarusintanakorn[1], Kittisak Sripha[1,2*]

[1] Department of Pharmaceutical Chemistry, Faculty of Pharmacy, Mahidol University, 447 Sri-Ayudhya Rd., Ratchathewi, Bangkok, Thailand
[2] Unit of Compounds Library for Drug Discovery, Faculty of Pharmacy, Mahidol University, 447 Sri-Ayudhya Rd., Ratchathewi, Bangkok, Thailand

ABSTRACT

This study explores novel compounds derived from indomethacin, a nonsteroidal anti-inflammatory drug (NSAID), using several approaches. Molecular docking techniques were employed to assess the interaction potential of 35 NSAIDs with key molecular targets involved in amyloid beta (Aβ) aggregation, a critical process in Alzheimer's disease pathogenesis. Notably, amtolmetin guacil, indomethacin, lornoxicam, and meloxicam exhibited significant docking orientations with two key Aβ fragments, $Aβ_{17-42}$ (2BEG) and $Aβ_{25-35}$ (1QWP), which are crucial binding sites on the Aβ peptide. *In vitro* experiments evaluated the ability of six NSAIDs to inhibit Aβ aggregation through ThT flavin assays. Indomethacin emerged as the prototype molecule for developing a novel anti-aggregation agent targeting Aβ due to its strong binding affinities along with effective inhibitory activity. Subsequently, 13 designed compounds were examined for their binding affinities at 2BEG and 1QWP, using parameters similar to NSAIDs. Among them, B2 and B4 demonstrated notable binding affinities and interactions with critical residues indicating their potential as anti-Aβ aggregation agents. Molecular dynamic simulation studies confirmed the stability of these complexes. *In silico* analysis of CNS permeation indicated the capability of compounds in the B series, notably B3 and B4, to be across the BBB. These findings illuminate the potential of indomethacin-derived compounds as promising candidates for further development as therapeutics targeting Aβ aggregation in Alzheimer's disease. Moreover, these investigations are expected to aid in the design and creation of new small molecules possessing anti-Aβ aggregation properties.

Keywords:
Anti-amyloid beta aggregation, Non-steroidal anti-inflammatory drugs (NSAIDs), Molecular docking, Alzheimer's disease

1. INTRODUCTION

Alzheimer's disease (AD) stands as the most prevalent form of progressive dementia among individuals aged 65 and older[1]. The primary manifestation of AD involves reduced acetylcholine levels, resulting in memory and learning deficits[2]. The main pathological hallmarks include the presence of amyloid plaques and neurofibrillary tangles (NFTs). These plaques result from the aggregation of amyloid beta (Aβ)[3], which is a peptide that plays a significant role in the pathogenesis of Alzheimer's disease. It is a fragment derived from the larger amyloid precursor protein (APP). The two main forms of amyloid beta are $Aβ_{40}$ and $Aβ_{42}$, with $Aβ_{42}$ being more prone to aggregation and considered more toxic. NFTs arise from the hyperphosphorylation of tau proteins that typically stabilize microtubules during mitosis. Both amyloid plaques and NFTs work synergistically to trigger neuronal cell death[4-5]. The production of Aβ occurs in different lengths by cleaving the amyloid precursor protein (APP). While the majority (~85-95%) is composed of 40-residue Aβ (Aβ40), a minor portion (~5-15%) consists of the 42-residue form (Aβ42). The cleavage of APP follows two pathways: the amyloidogenic pathway generates Aβ through β- and γ-secretase enzymes, while the non-amyloidogenic pathway leads to p3 formation via α- and γ-secretase enzymes[6-7].

***Corresponding author:**
*Kittisak Sripha Email: kittisak.srp@mahidol.ac.th

The Aβ monomer sequence comprises two prominent sections: a hydrophobic core encompassing amino acid sequences 17-21 and 29-42, and a hydrophilic region spanning sequence 22-28. Enzymatic degradation can eliminate this form. Upon aggregation into an insoluble state, Aβ adopts secondary structures, either β-sheet or amyloid fibrils, exhibiting two patterns: anti-parallel (intra-molecular β-strands) or parallel (inter-molecular β-sheets). These patterns rely on hydrogen bonding, salt bridges, and hydrophobic interactions to stabilize the structure. These interactions are driven by CO-NH bonds involving amino acid sequences like Asp23/Lys28 and Leu17-Ala21, or Gly29-Met35. Longer Aβ peptides like Aβ42 can form more stable oligomers and plaques due to interactions between Met35 and Gly37, in contrast to shorter peptides like Aβ40 which feature Met35 interacting with Gly33[8-11]. Notably, the p3 peptide, spanning amino acids 17-40, can also aggregate and damage the brain[12].

Currently, drugs used for AD only provide limited progression slowdown, including acetylcholine esterase inhibitors (AChEIs), N-methyl-D-aspartate (NMDA) antagonists, and nicotinic agonists[13]. Consequently, researchers seek alternative targets to halt disease progression, such as inhibiting enzymes β- and γ-secretase that are vital for Aβ production, or targeting Aβ aggregation and inflammation[14-15]. The role of chronic brain inflammation in AD is suggested due to its connection with neurodegeneration. Some non-steroidal anti-inflammatory drugs (NSAIDs) have been explored for their potential in this context. However, the precise mechanisms underlying NSAID-mediated neuroprotection remain unclear. Potential explanations include the suppression of chronic inflammatory responses in microglia and astrocytes, reduced neuronal expression of cyclooxygenase enzymes, or even the suppression of other AD-related mechanisms like Aβ and γ-secretase activity[16-18]. Recently, certain NSAIDs have shown potential in combating Aβ aggregation or modulating γ-secretase enzyme activity[19-20]. Indomethacin, ibuprofen, and naproxen are among the well-studied NSAIDs that have exhibited anti-Aβ aggregation effects both *in vitro* and in animal models. These compounds appear to alter Aβ fibrillogenesis and disrupt the formation of toxic Aβ oligomers, which are implicated in neuronal damage. However, the precise molecular mechanisms by which NSAIDs modulate Aβ aggregation remain a subject of ongoing investigation. Furthermore, the effects of NSAIDs on Aβ aggregation might extend beyond direct interactions. Notably, the binding of R-flurbiprofen to Aβ at the Gly25-Val36 amino acid position indicates their capacity to act as anti-aggregation agents[19-20]. Inflammation is closely linked to neurodegenerative processes, and NSAIDs' anti-inflammatory properties could indirectly impact Aβ accumulation and aggregation by mitigating inflammatory responses in the brain, as indicated in the report of Strohmeyer[21]. In recent years, there has been a shift toward exploring novel NSAID derivatives or analogs with enhanced selectivity for targeting Aβ aggregation pathways while minimizing potential adverse effects. Computational approaches, including molecular docking and structure-based design, have contributed to identifying new compounds that could exhibit improved anti-Aβ aggregation properties. In the study of neurodegenerative diseases, especially Alzheimer's disease and Aβ aggregation research, curcumin[22], a natural compound, emerges as one of the most powerful agents for combating Aβ aggregation in the *in vitro* experiments. Moreover, it exhibits a protective effect on neuroblastoma cells, shielding them from Aβ-induced cell death. As a result, many researchers in this field utilize curcumin as a standard reference in their investigations.

In light of these hypotheses, our investigation aims to elucidate the mechanisms behind NSAIDs' anti-aggregation effects through molecular docking techniques. We aim to provide a template for developing novel, promising anti-aggregation ligands. To confirm the findings from the docking study, the anti-aggregation properties of select NSAIDs are evaluated. Curcumin was used as a standard reference in this investigation.

2. MATERIALS AND METHODS

Based on the hypotheses above, our research endeavor involves examining the binding patterns of 35 NSAIDs and curcumin (Figure 1) to the Aβ peptide using molecular docking techniques. Our aim is to not only gain insights into the interaction mechanisms but also to establish a framework for designing new and prospective anti-aggregation ligands. All chemicals were purchased from commercial suppliers and utilized without undergoing any purification processes. The Faculty of Pharmacy's Department of Pharmaceutical Chemistry at Mahidol University provided support for NSAIDs employed in the *in vitro* test. Amyloid beta ($A\beta_{1-42}$) was acquired from the American Peptide Company in Sunnyvale, California, USA. The absorption values were measured using a Microplate reader (Fluorescence), the Spectra Max GeminiEM from USA.

2.1. Preparation of ligands and targeted macromolecule

The selection of ligands encompassed a collection of NSAIDs and curcumin, as depicted in Figure 1. These molecules were drawn, hydrogen atoms were added, and their energy was minimized using the Sybyl 8.1 program[23]. Energy minimization employed the Gasteiger-Huckel method with a gradient set to 0.05 kcal/mol.

The $A\beta_{17-42}$ and $A\beta_{25-35}$ peptides, serving as the targeted macromolecules, were previously resolved by Lührs et al.[8] and D'Ursi et al.[24], respectively (pdb codes: 2BEG and 1QWP). These peptide structures were obtained from

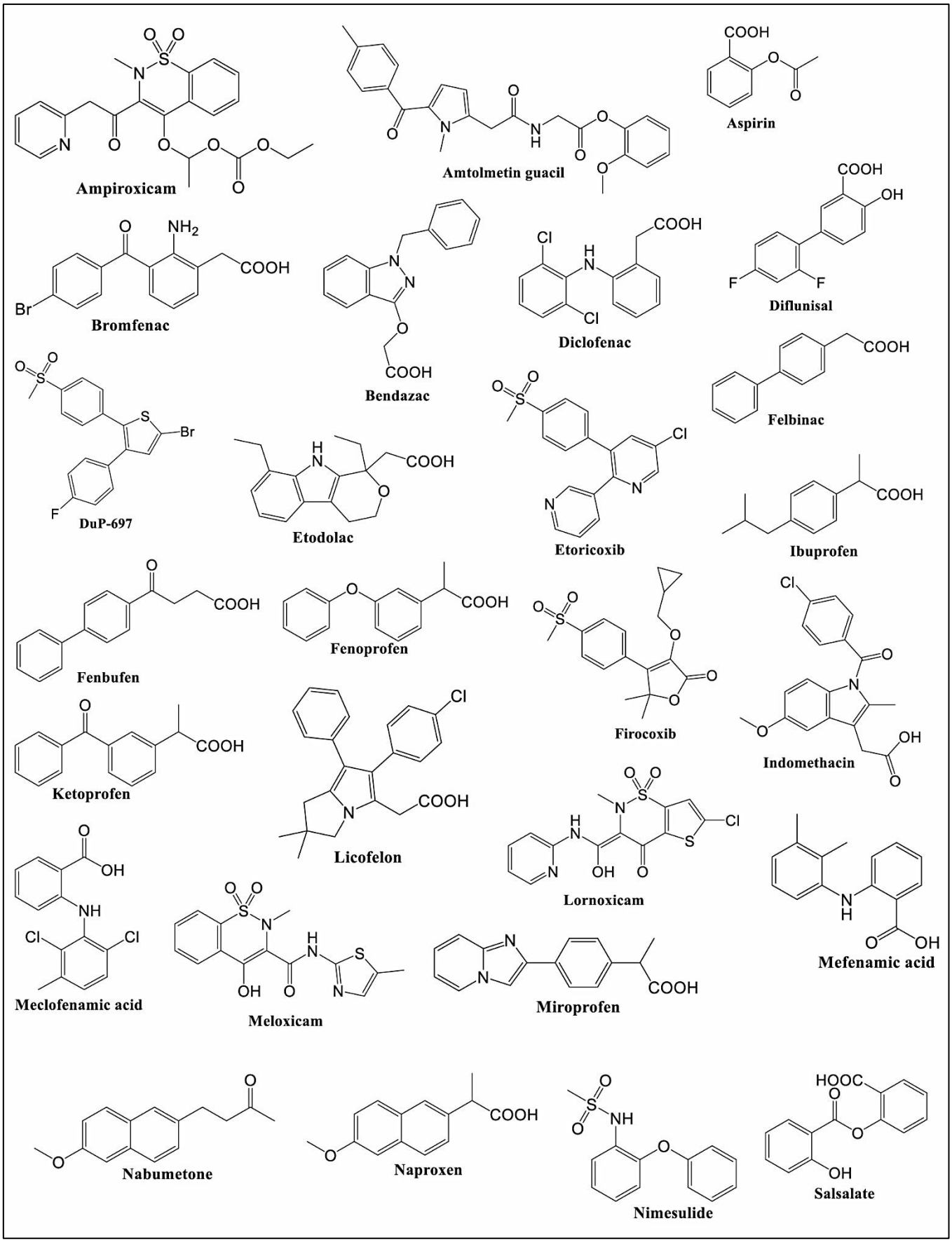

Figure 1. Structures of NSAIDs and curcumin.

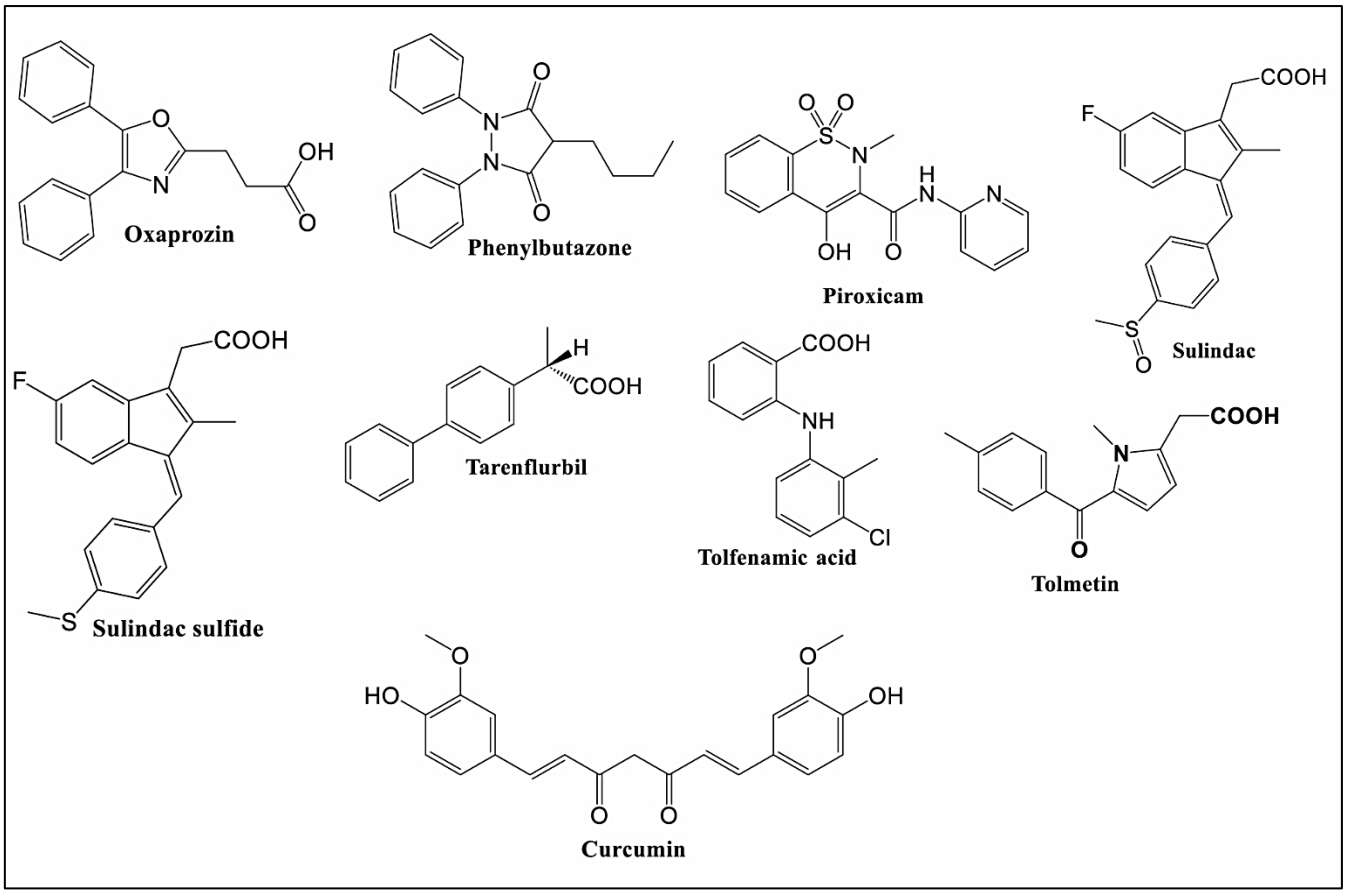

Figure 1. Structures of NSAIDs and curcumin. (cont.)

the Protein Data Bank and subsequently prepared in pdbqt format using the Autodock program 4.0[25]. The preparation process included the addition of all hydrogen atoms and Gasteiger charges.

A grid map was generated to cover the monomer fragments $A\beta_{17-42}$ and $A\beta_{25-35}$, employing a grid point spacing of 0.375 Å. This grid was centered on the core of the Aβ fibril. To execute the docking process, one hundred individual docking runs were undertaken utilizing the Lamarckian Genetic Algorithm (LGA) from the software package[26]. The population size was set at 150 for these runs. Within Autodock 4.0, various parameters were adjusted to establish the optimal conditions for ligand-protein docking. These parameters encompassed the maximum number of energy evaluations per docking run and grid volume. The maximum energy evaluations were capped at 4 million per run.

For $A\beta_{17-42}$ and $A\beta_{25-35}$, grid box sizes of 128x70x50 Å and 48x48x48 Å were set, respectively. All other parameters were maintained at their default settings. Docking outcomes with positional root-mean-square deviations (RMSD) differing by less than 2 Å were clustered and represented by the docking result boasting the most favorable free energy. The Aβ fibril was held in a fixed position throughout the docking process, while the flexible ligands underwent conformational exploration and docking. Subsequent analysis of the docking results was conducted using AutoDock Tools[27].

2.2. Evaluation of anti-aggregation activity (Thioflavin T Fluorescence Assay: ThT assay)

$A\beta_{1-42}$ salt was dissolved in 10 mM sodium hydroxide and then diluted in 50 mM Tris-HCl (pH 7.4) to create a stock solution at 25 µM. Stock solutions of six NSAIDs (diclofenac, ibuprofen, indomethacin, mefenamic acid, naproxen, piroxicam) and a positive control (curcumin) were prepared using DMSO. Each compound was further diluted in 50 mM Tris-HCl (pH 7.4) to achieve concentrations ranging from 0.01 to 1,000 µM, comprising six concentration points.

A total of 1 µL of each sample solution was added to 96-well plates. Each concentration point was prepared in triplicate, and a reagent blank was included in the setup. Subsequently, 9 µL of the 25 µM $A\beta_{1-42}$ stock solution was added to each well. The plate was then incubated in darkness at room temperature for 48 hours without agitation. Following the incubation, 200 µL of 5 µM ThT (Thioflavin T) in 50 mM Tris-HCl (pH 7.4) was introduced to each well. Fluorescence readings were taken using a SpectraMax GEMINI EM dual scanning microplate spectrofluorometer from Molecular Devices, Sunnyvale, CA, USA. The excitation and emission wavelengths were set at 446 nm and 500 nm, respectively[28]. The anti-aggregation percentage was determined through the formula: [1-(Fsample-Fblank)/Fcontrol]×100. Here Fsample represents the fluorescence reading of the sample, Fblank

is the fluorescence reading of the reagent blank, and Fcontrol signifies the fluorescence reading of the control.

2.3. Molecular Dynamics (MD) Simulation

The optimization of the complexes between the designed compounds and the $A\beta_{1-42}$ peptide was conducted through Molecular Dynamics (MD) simulation employing the NAMD software[29] and utilizing the CHARMM force field[30]. The complexes were immersed in a TIP3P model water box, and the system's charge was neutralized with an appropriate number of counter ions. Initially, the water box underwent minimization using the conjugate gradient method. Before the MD simulation, a system equilibration for 200 ps occurred in the NPT ensemble at 310 K and 1 atm, controlled by the Nosé-Hoover Langevin piston method with 2 fs time steps and the SHAKE algorithm. Periodic boundary conditions (PBC) and the Particle Mesh Ewald (PME) method were applied for calculations. The production steps extended for 60 ns, and the stability was assessed using root mean square deviation (RMSD). Finally, the interactions within the complexes were analyzed using BIOVIA Discovery Studio Visualizer 2020[31].

3. RESULTS AND DISCUSSION

In the initial step of our investigation, we begin by evaluating the potential anti-aggregation effects using a docking approach involving fragment $A\beta_{17-42}$ (known as 2BEG). This model was created using a hydrogen/deuterium-exchange NMR technique as elucidated by Lührs and coworkers[8], which suppresses the exchange process. However, there are still unspecified areas within the Asp1-Lys16 region. The remaining segments are of great importance for the formation of fibrils. A structural arrangement characterized by β-strand-turn-β-strand is observed between residues Val18-Ser26 (referred to as β1) and Ile31-Ala42 (referred to as β2). Based on the NMR data, they observed interactions within the β-sheet involving Asp23/Lys28 (forming a salt bridge interaction), Phe19/Gly38, and Ala21/Val36[8].

To explain the potential inhibition of $A\beta_{1-42}$ aggregation by NSAIDs, we utilize molecular docking simulations. These simulations allow us to elucidate the specific molecular interactions involved. Through the integrated

Table 1. Results docking of curcumin and NSAIDs with 2BEG.

Drug	HP	BE (kcal/mole)	HA	HD
Curcumin	Phe19,Ala21-Asp23,Leu34,Val36-Val40	-5.77	OH:Asn23,CO:Gly37,OCH3:Val39	No
Ampiroxicam	Phe19,Ala21,Leu34,Val36-Val40	-7.92	SO_2:Val39,CO:Ala21,Gly37	No
Amtolmetin guacil	Phe19,Ala21-Asp23,Leu34-Gly38	-8.51	CO:Gly37	No
Aspirin	Phe19,Gly37-Val40	-3.82	O:Val39	No
Bendazac	Phe19-Glu22,Val36	-6.11	O:Ala21	No
Bromfenac	Glu22,Asp23,Gly33-Val36	-6.20	CO:Met35	NH:Met35
Diclofenac	Phe19,Ala21,Val36-Val39	-5.94	OH:Ala21	No
Diflunisal	Phe19,Ala21,Gly37-Val39	-5.45	OH:Val39	No
DuP-697	Phe19,Ala21,Met35-Gly38,Val40	-6.49	SO_2:Ala21	No
Etodolac	Phe19,Ala21,Val36-Gly38,Val40	-6.27	OH:Ala21	No
Etoricoxib	Phe19,Ala21,Val36,Gly37,Val40	-6.33	N:Gly37	No
Felbinac	Phe19,Ala21-Asp23,Leu34	-4.46	OH:Ala21	No
Fenbufen	Phe19,Ala21,Leu34,Val36-Val39	-5.68	OH:Val39	No
Fenoprofen	Glu22,Asp23,Gly33-Val36	-5.35	OH:Met35	No
Firocoxib	Asp23,Gly33-Gly37	-6.30	O:Met35,SO_2:Gly37	No
Ibuprofen	Ala21-Asp23,Gly33-Met35	-4.60	OH:Met35	No
Indomethacin	Phe19,Ala21,Asp23,Leu34,Val36	-7.30	OH:Asp23	No
Ketoprofen	Ala21,Asp23,Leu34	-5.86	CO:Asp23	No
Licofelone	Ala21,Glu22,Leu34-Gly37	-6.46	OH:Met35	No
Lornoxicam	Ala21,Asp23,Ile32-Val36	-7.07	OH:Met35	NH:Gly33
Meclofenamic acid	Phe19,Ala21,Val36-Val40	-5.94	No	No
Mefenamic acid	Ala21-Asp23,Leu34,Val36	-5.48	OH:Asp23	No
Meloxicam	Phe19,Met35-Gly37,Val39,Val40	-7.23	N:Gly37,SO_2:Val39	No
Miroprofen	Phe19,Ala21,Gly37,Val39	-6.04	OH:Ala21	No
Nabumetone	Phe19,Ala21-Asp23,Leu34,Val36	-4.72	CO:Ala21	No
Naproxen	Phe19,Ala21,Gly37-Val40	-5.99	OH:Ala21,CH_3O:Val39	No
Nimesulide	Phe19-Ala21	-5.28	PhO:Ala21	NH:Phe19
Oxaprozin	Ala21,Glu22,Gly33-Gly37	-6.11	OH:Met35	No
Phenylbutazone	Phe19,Gly37-Val40	-5.58	No	No
Piroxicam	Phe19,Met35,Gly37,Val39,Val40	-6.37	SO_2:Val39	NH:Gly37
Salsalate	Glu22,Asp23,Gly33-Val36	-5.80	CO:Met35	No
Sulindac	Phe19,Ala21,Val36-Val39	-6.74	OH:Gly37	No
Sulindac sulfide	Phe19,Met35-Val40	-6.00	OH:Val39	No
Tarenflurbil	Ala21,Glu22,Gly33-Val36	-4.99	OH:Met35	No
Tolfenamic acid	Phe19,Ala21,Val36,Gly37,Val39,Val40	-6.68	OH:Ala21	No
Tolmetin	Ala21-Asp23,Leu34-Val36	-5.64	OH:Met35	No

clustering method, we identify the lowest energy complex with the highest occurrence as the most stable configuration between NSAIDs and the Aβ complex. A total of 35 NSAIDs and curcumin were examined to explore potential anti-aggregation mechanisms. The docking results were assessed based on their positioning during docking and their binding energy (BE) within the monomeric $A\beta_{17-42}$ peptide derived from 2BEG. These findings are consistent with a prior study that identified anti-aggregation properties in certain NSAIDs (Table 1).

Table 1 illustrates the amino acids that interact with NSAIDs through various types of interactions, such as hydrogen bonding acceptors (HA), hydrogen bonding donors (HD), and hydrophobic (HP) interactions. In the docking experiment, NSAIDs exhibit anti-aggregation activity by binding to sites via hydrogen bonds and hydrophobic interactions. Significantly, ampiroxicam, amtolmetin guacil, indomethacin, lornoxicam, and meloxicam exhibit notable docking orientations, revealing binding affinities of -7.92, -8.51, -7.30, -7.07, and -7.23 kcal/mol, respectively. These interactions primarily take place at the active sites Phe19/Gly38 and/or Ala21/Val36 across all these NSAIDs. Notably, an additional interaction involving the salt bridge region (Asp23/Lys28) is exclusively observed in the cases of amtolmetin guacil, indomethacin, and lornoxicam (as illustrated in Figure 2 and Figure 3). On the other hand, felbinac, aspirin, ibuprofen, nabumetone, and tarenflurbil demonstrate less favorable docking orientations, exhibiting binding affinities of -4.46, -3.82, -4.60, -4.72, and -4.99 kcal/mol, respectively.

According to findings by Thomas and colleagues[32], R-flurbiprofen (known as Tarenflurbil) has an affinity for binding to the amino acid sequence 25-36. To explore the interaction between the ligand and the macromolecule, we initiated a docking process of Tarenflurbil with 2BEG. The results revealed an interaction at this specific site involving a hydrogen bond with the residue Met35. Additionally, hydrophobic interactions occurred within the vicinity of hydrophilic and hydrophobic residues Ala21, Glu22, and Gly33-Val36. These outcomes indicate

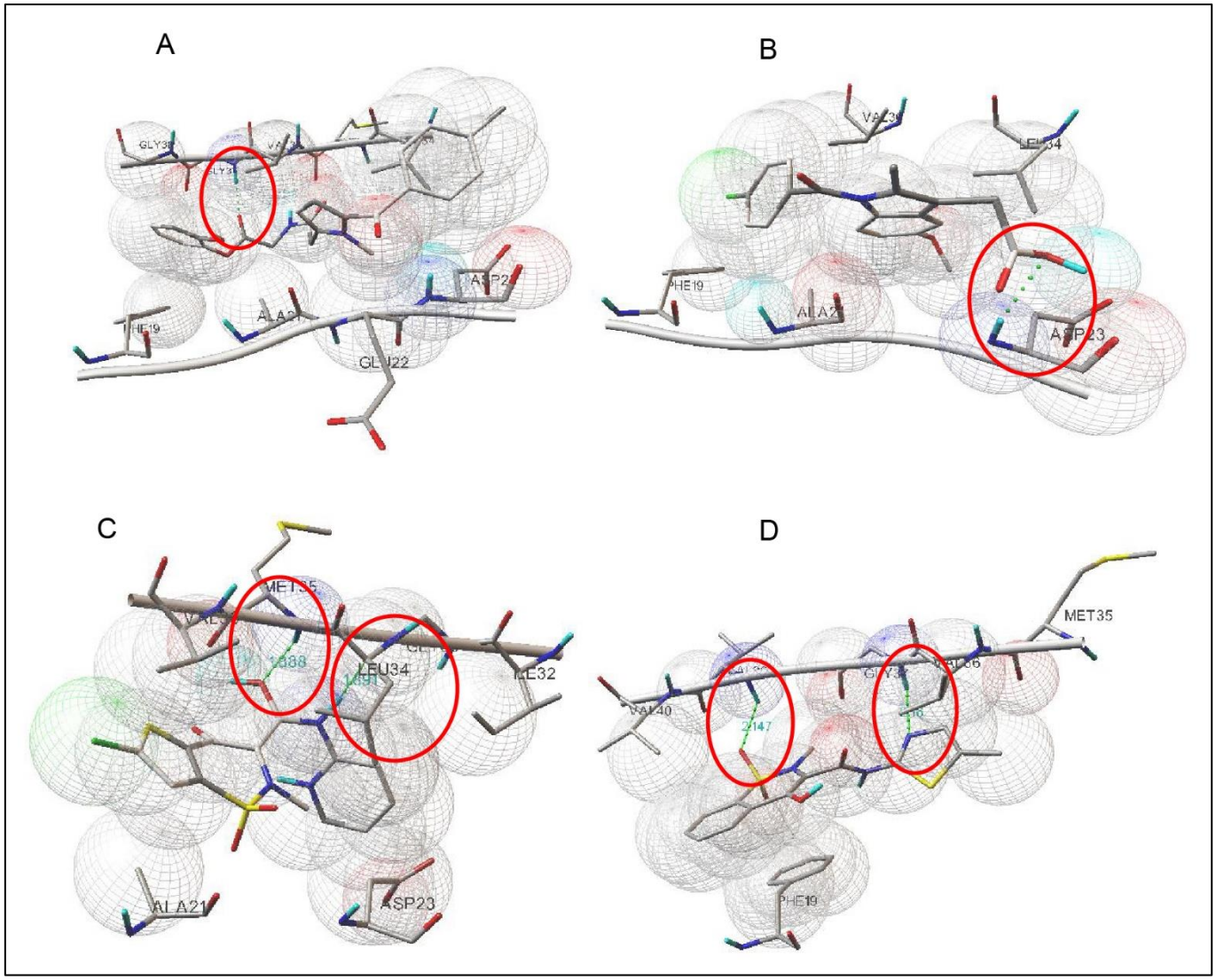

Figure 2. The docking orientations and interactions of (A) amtolmetin guacil, (B) indomethacin, (C) lornoxicam, and (D) meloxicam with $A\beta_{17-42}$ are represented by green dots, where the hydrogen bonds are indicated.

that under these circumstances, Tarenflurbil demonstrates a stronger inclination to bind with residues Gly25-Val36 (β2) rather than His13-Val24 (β1). In the case of β1, binding occurs solely through a hydrophobic interaction with Ala21 and Glu22. However, in the case of β2, there is a hydrophobic interaction with Gly33-Val36 and a hydrogen bond with Met35, which appears to be stronger than the hydrophobic interaction.

The previous study suggested that fragment containing Gly25-Met35 residues of $A\beta_{42}$ shows the shortest fragment that can be a critical site for producing aggregated structure and cause toxicity[24]. This fragment is composed of three major components that participate in both oligomer formation and aggregation. Specifically, these components correspond to the amino acid sequence spanning from 25 to 35, arranged in the form of a GxxxG motif. The majority of these constituents are hydrophobic, particularly residues 29-33 and 33-35, except for the polar component between residues 25 and 29[33]. As a result, our subsequent docking experiment employs this specific fragment $A\beta_{25\text{-}35}$ (1QWP) to validate the anti-aggregation efficacy of ligands identified in the initial step. This model was established through the application of nuclear magnetic resonance (NMR) and circular dichroism techniques[24]. The docking data is shown in Table 2.

The docking results for the $A\beta_{25\text{-}35}$ fragment reflect a comparable binding affinity trend to that observed for the $A\beta_{17\text{-}42}$ fragment. Among the 35 NSAIDs, amtolmetin guacil, indomethacin, lornoxicam, and meloxicam consistently demonstrate favorable results in terms of binding energy and binding mode when interacting with the $A\beta_{25\text{-}35}$ fragment. These compounds exhibit binding energies of -7.30, -7.46, -7.34, and -7.31 kcal/mol, respectively. On the contrary, compounds such as felbinac, aspirin, ibuprofen, nabumetone, tarenflurbil, and diflunisal demonstrate low binding energies of -4.65, -4.33, -4.47, -4.81, -5.17, and -4.86 kcal/mol, respectively. Observations reveal that specific amino acid residues, namely Ile31, Gly33, and Leu34 within the hydrophobic region, play a crucial role in forming hydrophobic interactions through van der Waals forces. Additionally, the majority of hydrogen bond interactions occur within the polar region spanning Gly25 to Gly29, excluding Ile31, which is uniquely found in lornoxicam and meloxicam. Interestingly, lornoxicam and meloxicam establish interactions within both the polar and hydrophobic regions (Figure 3). Considering

Table 2. Results docking of curcumin and NSAIDs with 1QWP.

Drug	HP	BE (kcal/mole)	HA	HD
Curcumin	Lys28,Ile31,Ile32,Leu34,Met35	-4.38	No	OH:Met35
Ampiroxicam	Asn27,Ala30-Leu34	-6.36	SO_2:Asn27,CH_2O:Ala30	No
Amtolmetin guacil	Asn27-Leu34	-7.30	No	No
Aspirin	Asn27,Ile31,Gly33,Leu34	-4.33	No	No
Bendazac	Ser26,Asn27,Ala30-Leu34	-5.98	CO:Ser26,OH:Asn27	No
Bromfenac	Ala30-Met35	-6.44	No	NH_2:Leu34,Met35
Diclofenac	Asn27,Ala30-Leu34	-5.07	No	NH:Ala30
Diflunisal	Asn27,Ala30,Ile31,Leu34,Met35	-4.86	No	No
DuP-697	Ser26, Ala30-Leu34	-4.92	No	No
Etodolac	Asn27,Ile31-Leu34	-5.03	OH:Asn27	No
Etoricoxib	Lys28,Ile31,Gly33,Leu34	-5.04	No	No
Felbinac	Ala30-Met35	-4.65	No	No
Fenbufen	Ser26,Lys28-leu34	-5.23	OH:Lys28	No
Fenoprofen	Asn27,Ala30-Met35	-5.41	No	No
Firocoxib	Ile31,Gly33,Leu34	-5.02	CH_2O:Leu34	No
Ibuprofen	Ala30-Leu34	-4.47	No	No
Indomethacin	Ser26-Lys28,Ile31,Gly33,Leu34	-7.46	CH_3O:Asn27,OH:Lys28	No
Ketoprofen	Ser26,Lys28,Ile31,Leu34	-4.97	OH:Lys28	No
Licofelone	Ser26,Asn27,Ala30-Met35	-5.49	OH:Asn27	No
Lornoxicam	Lys28-Met35	-7.34	No	CHNH,CH_2NH:Ile31
Meclofenamic acid	Asn27,Ala30-Leu34	-5.05	No	NH:Ala30
Mefenamic acid	Asn27,Ala30-Met35	-5.53	No	No
Meloxicam	Asn27,Ala30,Ile31,Leu34	-7.31	SO_2:Asn27	OH:Ile31
Miroprofen	Ala30-Leu34	-5.34	No	No
Nabumetone	Lys28-Leu34	-4.81	CO:Lys28	No
Naproxen	Ser26,Lys28,Ile31,Gly33,Leu34	-5.29	CO:Lys28	No
Nimesulide	Asn27,Ile31,Gly33,Leu34	-5.55	SO_2:Asn27	NH:Asn27
Oxaprozin	Ser26,Asn27,Ala30-Met35	-5.59	No	No
Phenylbutazone	Asn27,Ala30-Leu34	-5.52	No	No
Piroxicam	Asn27,Ala30,Ile31,Leu34	-6.35	SO_2:Asn27	No
Salsalate	Asn27,Ile31-Met35	-5.59	No	No
Sulindac	Ser26,Asn27,Ile31-Leu34	-6.00	OH:Ser26,CO:Asn27	No
Sulindac sulfide	Ser26,Lys28,Ile31,Leu34,Met35	-5.51	OH:Lys28	No
Tarenflurbil	Ser26,Lys28,Ile31,Leu34	-5.17	OH:Lys28	No
Tolfenamic acid	Asn27,Ala30-Leu34	-5.53	No	NH:Ala30
Tolmetin	Ser26-Leu34	-5.59	CO:Lys28	No

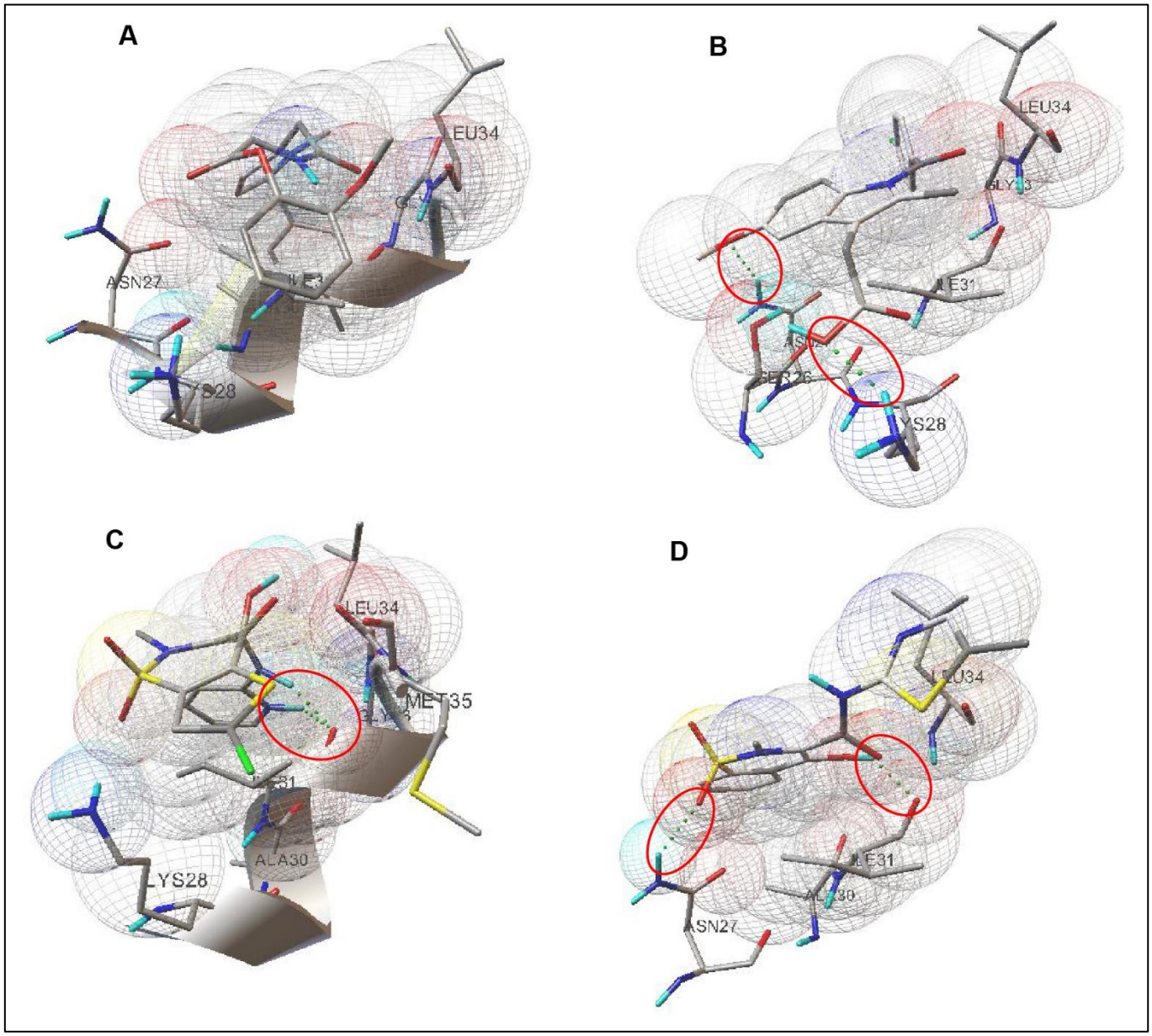

Figure 3. Docking positioning and interaction of (A) Amtolmetin guacil (B) Indomethacin (C) Lornoxicam (D) Meloxicam with $A\beta_{25-35}$. The H-bond is depicted as green dots.

the binding affinities observed for both the $A\beta_{17-42}$ and $A\beta_{25-35}$ fragments, it is reasonable to suggest that the aforementioned four NSAIDs could potentially exhibit anti-aggregation activity. Our experiment demonstrated the attachment of curcumin to both fragments indicating a hydrophobic interaction with the salt bridge region (Asp23/Lys28) (Table 1 and Table 2). These results are consistent with the finding of Mithu and colleagues[34], suggesting that curcumin binding to the salt bridge region disrupts the intermolecular arrangement of Aβ peptide, thereby interfering with the fibrillar formation. Nevertheless, it was observed that the binding energy of curcumin complexes was less than that of the four NSAIDs candidates, with binding energies of -5.77 kcal/mol for 2BEG and -4.38 kcal/mol for 1QWP, respectively.

According to the anticipated activity from docking analysis, the structure-activity relationships (SARs) align with the findings of Azam[35] who observed that a pair of aryl or hetero-aryl ring systems connected by a linker demonstrated significant affinity to the Aβ protein. Linkers with polar characteristics, like ether, carbonyl, amine, or amide groups, were found to enhance binding affinity.

The inhibitory effect on aggregation by $A\beta_{42}$ was assessed for six NSAIDs: diclofenac, ibuprofen, indomethacin, mefenamic acid, naproxen, and piroxicam. The Thioflavin T assay was employed to assess inhibitory potencies, quantified through IC_{50} values. Curcumin was used as a positive control in this test (Figure 4).

As shown in Figure 4, among the set of six NSAIDs that were tested, mefenamic acid demonstrated significant potential in inhibiting the aggregation of Aβ protein, with an IC_{50} of 0.90±2.44 μM. However, this finding contradicts the results of the docking analysis. Consequently, indomethacin was chosen as the prototype molecule for

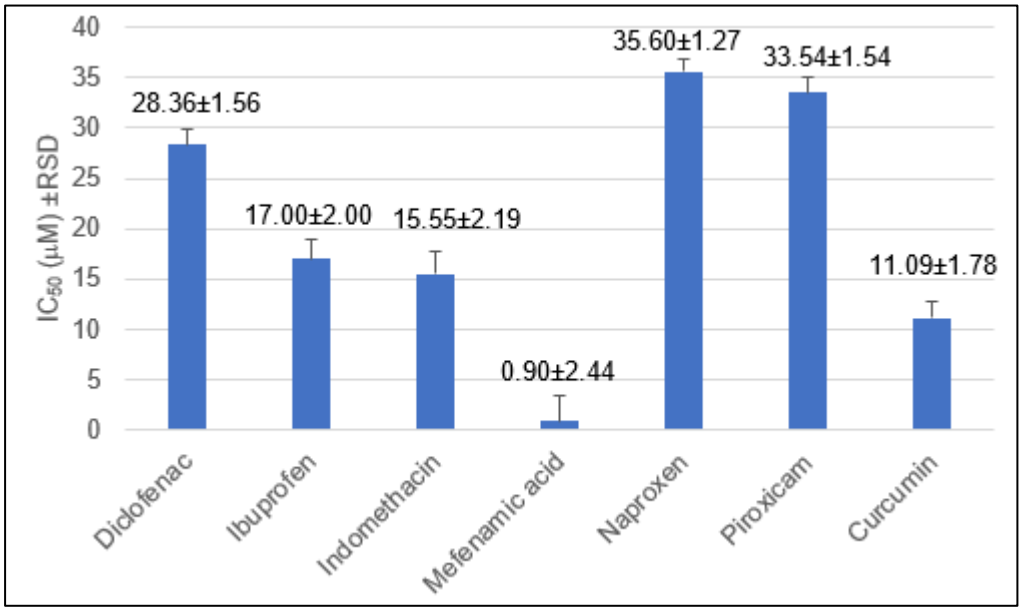

Figure 4. Anti-aggregation action of six NSAIDs on $A\beta_{42}$ shown as IC_{50}.

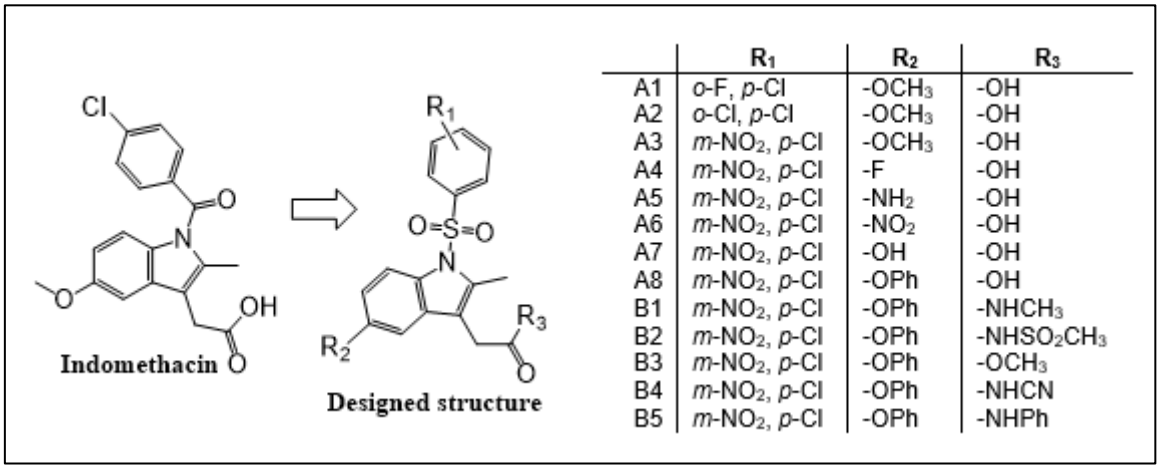

	R_1	R_2	R_3
A1	*o*-F, *p*-Cl	$-OCH_3$	-OH
A2	*o*-Cl, *p*-Cl	$-OCH_3$	-OH
A3	*m*-NO_2, *p*-Cl	$-OCH_3$	-OH
A4	*m*-NO_2, *p*-Cl	-F	-OH
A5	*m*-NO_2, *p*-Cl	$-NH_2$	-OH
A6	*m*-NO_2, *p*-Cl	$-NO_2$	-OH
A7	*m*-NO_2, *p*-Cl	-OH	-OH
A8	*m*-NO_2, *p*-Cl	-OPh	-OH
B1	*m*-NO_2, *p*-Cl	-OPh	$-NHCH_3$
B2	*m*-NO_2, *p*-Cl	-OPh	$-NHSO_2CH_3$
B3	*m*-NO_2, *p*-Cl	-OPh	$-OCH_3$
B4	*m*-NO_2, *p*-Cl	-OPh	-NHCN
B5	*m*-NO_2, *p*-Cl	-OPh	-NHPh

Figure 5. Designed structures derived from indomethacin.

the development of a new active anti-aggregation agent targeting Aβ. This selection was based on its strong binding affinities, indicated by binding energies of -7.30 kcal/mol for 2BEG and -7.46 kcal/mol for 1QWP, as well as its effective inhibitory activity with an IC_{50} of 15.55± 2.19 μM. Based on the findings from the docking investigation and the evaluation of anti-aggregation activity, indomethacin was selected as the active model. To enhance its activity, it was recognized that making adjustments at the R_2 and R_3 positions of indomethacin was essential to introduce H-bond into the Asp23/Lys28 region of the $A\beta_{1\text{-}42}$ peptide. This region is pivotal in the formation of fibrils and plaques. Following this, we modified the R_2 and R_3 substitution, alongside R_1 as depicted in Figure 5. Subsequently, a new set of docking simulations was carried out, utilizing the same parameters and methodology as outlined in section 2.1. The docking results are shown in Table 3 and Table 4.

According to Table 3, we conducted the docking simulation of all the designed compounds with $A\beta_{25\text{-}35}$ (1QWP), revealing that substituting the carbonyl group with sulfone and altering the methoxy group to phenoxy in the R_2 position resulted in an increased binding affinity. Introducing electron-withdrawing groups (R_1) like Cl and NO_2 to the aromatic ring led to improved binding energies. Remarkably, introducing modifications at the R_3 position involving ester, amide, or sulfonamide derivatives while maintaining a phenoxy group at R_2 led to a substantial enhancement in binding affinities. Furthermore, changing the R_3 acid group to sulfonamide and cyanamide derivatives led to superior binding energies. This effect is exemplified by compounds B2 and B4, displaying binding energies of -8.96 kcal/mol and -8.35 kcal/mol, respectively. Similarly, these two designed compound derivatives demonstrated strong interaction with $A\beta_{17\text{-}42}$ (2BEG), as evidenced by binding energies of -8.94 kcal/mol and -9.13 kcal/mol, respectively (Table 4). Recently, a phenoxyindole scaffold has been derived from indomethacin, aiming to serve as a neuroprotective agent. Surprisingly, a recent report highlighted the promising

Table 3. Binding energy and interaction of modified structure indomethacin with 1QWP.

Compound	Structure	BE (kcal/mole)	H-bond	Cluster
Indomethacin	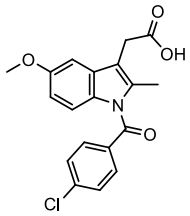	-7.30	2 acceptor CH_3O : Asn27 OH(3) : Lys28	84
A1	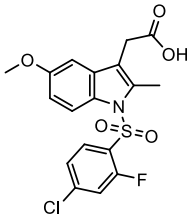	-6.38	2 acceptor CH_3O : Asn27 OH(3) : Lys28	20
A2	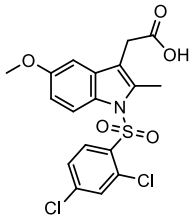	-5.77	2 acceptor CO : Ser26 OH(3) : Asn27	16
A3	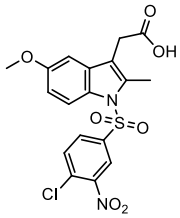	-7.36	2 acceptor CH_3O : Asn27 CO(3) : Lys28	16
A4	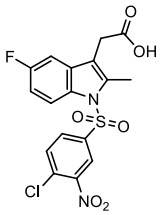	-7.2	2 acceptor CO : Ser26 OH : Asn27	10
A5	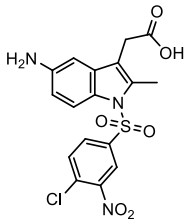	-6.34	1 acceptor NO_2 : Lys28	94
A6	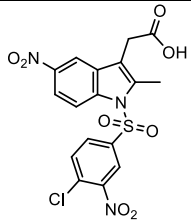	-6.67	2 acceptor NO_2(5) : Asn27 OH : Lys28	10
A7	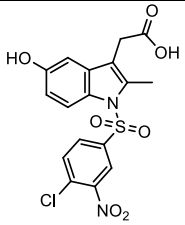	-7.20	2 acceptor OH(5) : Asn27 OH(3) : Lys28	15

Table 3. Binding energy and interaction of modified structure indomethacin with 1QWP. (cont.)

Compound	Structure	BE (kcal/mole)	H-bond	Cluster
A8	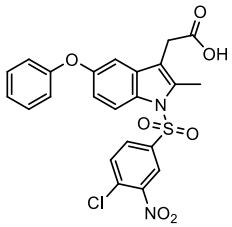	-7.65	2 acceptor PhO : Asn27 CO : Lys28	11
B1	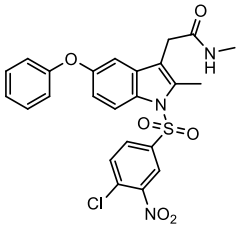	-7.96	3 acceptor CO : Ser26,Asn27 NO_2 : Lys28 1 donor NH : Ser26	48
B2	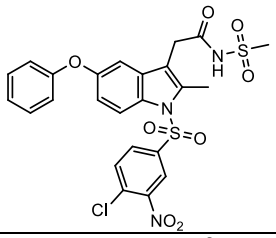	-8.96	1 acceptor PhO : Asn27	16
B3	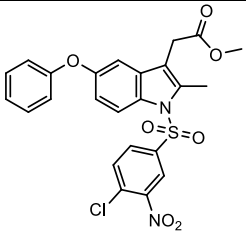	-7.99	3 acceptor CO : Ser26 PhO : Asn27 NO_2 : Lys28	82
B4	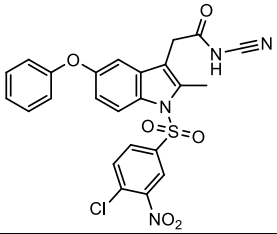	-8.35	2 acceptor PhO : Asn27 NO_2 : Lys28	20
B5	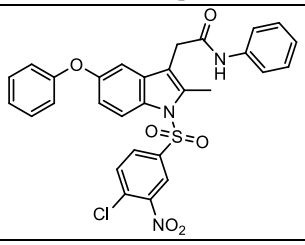	-7.76	2 acceptor PhO : Asn27 NO_2 : Lys28	36

Table 4. Binding energy and interaction of modified structure indomethacin with 2BEG.

Compound	Structure	BE (kcal/mole)	H-bond	Cluster
B1	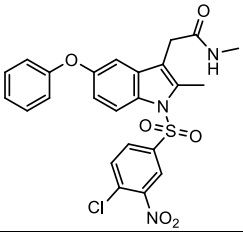	-8.45	1 acceptor NO_2 : Glu22 1 donor NH_2 : Gly37	19

Table 4. Binding energy and interaction of modified structure indomethacin with 2BEG. (cont.)

Compound	Structure	BE (kcal/mole)	H-bond	Cluster
B2	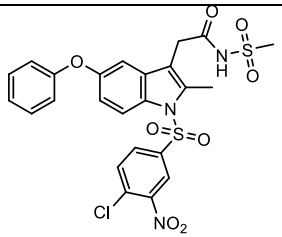	-8.94	2 acceptor NO_2 : Met 35 SO_2 : Gly 37	5
B3	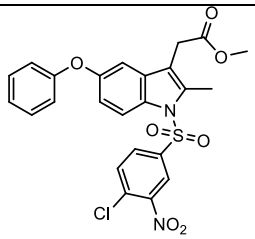	-7.99	2 acceptor NO_2 : Glu22 PhO : Gly37	30
B4	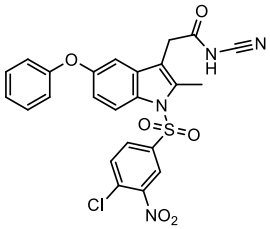	-9.13	1 acceptor NO_2 : Glu22	15
B5	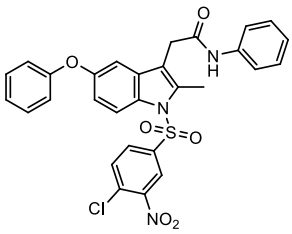	-8.55	1 acceptor CH_2CO : Gly37	28

potential of sulfonamide and cyanamide derivatives of phenoxyindole in combating Aβ aggregation and demonstrating antioxidant properties[36].

When comparing the binding mechanisms of indomethacin with those of compounds B2 and B4, it was evident that the methoxy group in indomethacin, along with the phenoxy groups in B2 and B4, engaged in hydrogen bonding interactions with Asn27 of the $A\beta_{25\text{-}35}$ fragment (1QWP). Furthermore, the nitro group in B4 and the hydroxy group in indomethacin exhibited hydrogen bonds with Lys28. Due to the electron-withdrawing properties inherent in phenoxy and nitro groups, B4 prominently exhibited strong H-bond acceptors for both Asn27 and Lys28. This observation provided substantial evidence for the robust binding affinity of B4 towards the $A\beta_{25\text{-}35}$ fragment. Figure 6 illustrates the binding interaction between compounds B2 and B4, on the $A\beta_{25\text{-}35}$ fragment. In the case of the $A\beta_{17\text{-}42}$ fragment (2BEG), the nitro and sulfone groups of B2 attached to Gly37 and Val39, respectively, while the nitro group of B4 bound to Glu22. The hydroxy part of the carboxylic group in indomethacin established an H-bond with Asp23.

To investigate the stability of the complex between monomeric Aβ peptide and compounds B2 or B4, which exhibited a high affinity binding, we conducted simulations for 60 ns to analyze the Root Mean Square Deviation (RMSD). Throughout the simulation, both the protein and ligands B2 or B4 remained stable within the 2 Å range. A comparison of binding mechanisms using molecular dynamics simulation revealed that compounds B2 and B4 exhibited a similar conformation to the $A\beta_{25\text{-}35}$ fragment (1QWP) as determined by Autodock 4.0. The MD analysis demonstrates that the compounds B2 and B4 still interacted on Aβ peptide at close to similar regions, particularly the binding of B4 on the $A\beta_{25\text{-}35}$ fragment (1QWP). Notably, the nitro group of B4 was in proximity to Lys28, the salt bridge region. The cyanamide group formed H-bond with Ser26 and the phenoxy group exhibited the pi-alkyl interaction with Leu34. In the case of B2, we noted the establishment of a hydrogen bond between the nitro group and Gly33/Leu34. Additionally, pi-alkyl interactions were observed between the phenyl ring and Leu34, as well as between the indole ring and Ile31. This finding supports the potential of compounds B2 and B4 to promote the inhibition of Aβ aggregation. Figure 7 depicts RMSD values and intermolecular interactions at equilibrium between $A\beta_{25\text{-}35}$ and compounds B2 and B4.

We employed GastroPlusTM software version 9.8 (Simulations Plus Inc., Lancaster, CA, USA)[37] to predict the blood-brain barrier (BBB) diffusion of all the modified

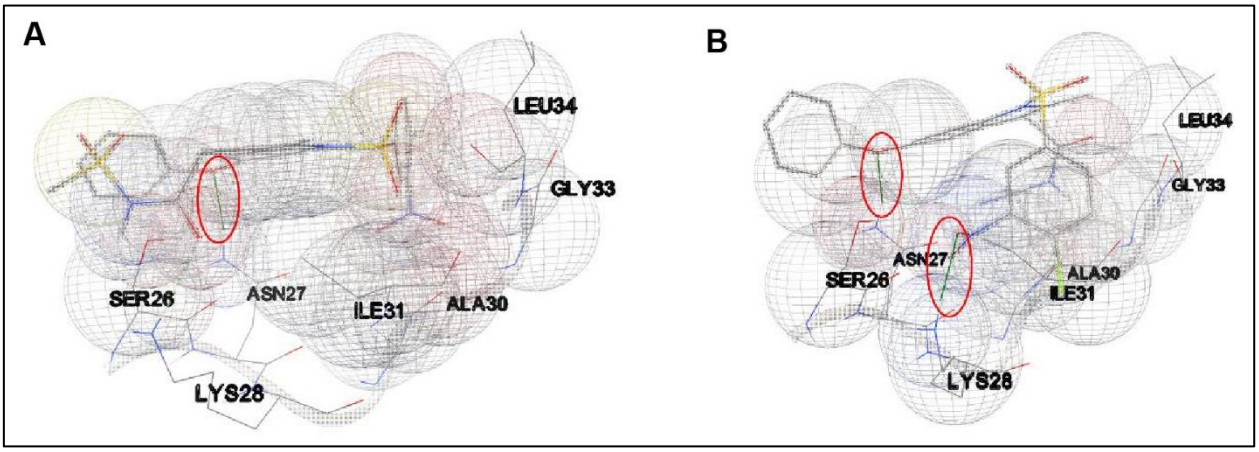

Figure 6. Docking positioning and interaction of (A) B2 and (B) B4 with $A\beta_{25\text{-}35}$. The H-bond is depicted as green dots.

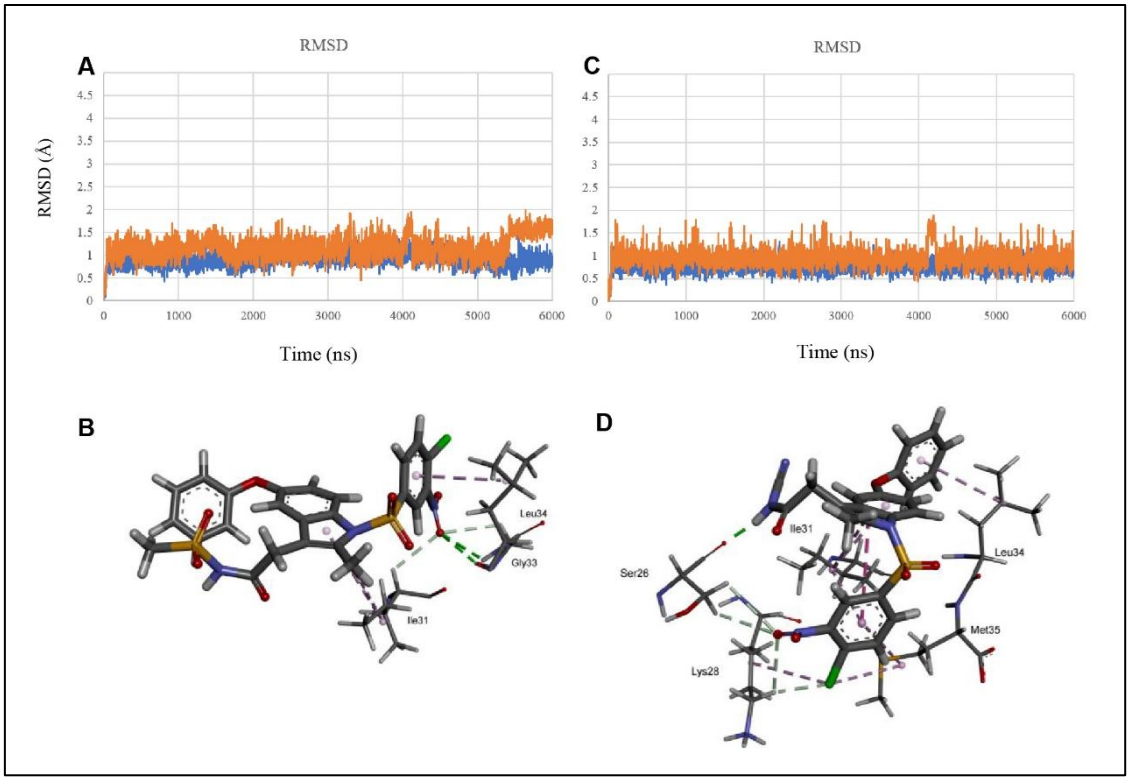

Figure 7. RMSD values and 3D interactions of the complex between monomeric $A\beta_{25\text{-}35}$ (1QWP) and compound B2 (A, B) and B4 (C, D), respectively.

structures derived from indomethacin. The prediction of physicochemical properties including the percentage of BBB penetration for these derivatives is presented in Table 5. In contrast to indomethacin, which displays the lowest penetration capacity, the B series demonstrates notably enhanced passive penetration across the BBB in comparison to the A series. Particularly, B3 and B4 exhibit a higher percentage of BBB penetration. This indicates that the replacement of carboxylic acid with a methyl ester (B3) or cyanamide (B4), along with the introduction of a non-polar substituted group, such as the phenoxy group at the 5-position of the indole ring, facilitates the passive penetration of the blood-brain barrier by the compounds. However, further structural improvements are needed to achieve increased BBB penetration.

4. CONCLUSION

In summary, the molecular docking study investigating the potential anti-Aβ aggregation effects of NSAIDs yields promising insights. The results suggest that certain NSAIDs, namely amtolmetin guacil, indomethacin, lornoxicam, and meloxicam, exhibit favorable binding interactions with Aβ peptides, particularly the $A\beta_{17\text{-}42}$ and $A\beta_{25\text{-}35}$ fragments linked to aggregation processes. *In vitro*, testing of six NSAIDs, diclofenac, ibuprofen, indomethacin, mefenamic acid, naproxen, and piroxicam, was conducted using the Thioflavin T assay to evaluate their anti-Aβ aggregation properties. The concurrence of findings between the docking study and *in vitro* testing supports the identification of indomethacin as a viable candidate model. Consequently, novel active compounds

Table 5. Prediction of physicochemical properties for modified structures of indomethacin.

Entry	LogP (neutral)	pH	Solubility (mg/mL)	% of BBB Penetration
Indomethacin	4.03	4.60	0.0107	3
A1	3.80	4.70	9.41×10^{-3}	10
A2	4.12	4.84	6.74×10^{-3}	3
A3	3.29	4.93	5.58×10^{-3}	10
A4	3.44	5.18	2.96×10^{-3}	10
A5	1.96	4.46	0.0246	10
A6	3.29	5.36	2.03×10^{-3}	3
A7	2.71	3.91	0.0974	3
A8	4.47	6.11	3.88×10^{-4}	3
B1	4.41	7.00	2.39×10^{-4}	16
B2	4.02	5.74	1.07×10^{-3}	10
B3	5.21	7.00	1.22×10^{-4}	38
B4	4.25	6.99	1.34×10^{-4}	26
B5	5.74	7.00	3.70×10^{-5}	10

were devised by modifying the indomethacin structure. Molecular docking was subsequently employed to validate the binding mechanism of these designed compounds. Particularly noteworthy is the substantial binding energy exhibited by compounds B2 and B4 in their interactions with $A\beta_{17\text{-}42}$ (2-BEG) and $A\beta_{25\text{-}35}$ (1QWP) fragments, with B4 notably at the salt bridge region, a crucial area for Aβ aggregation. Molecular dynamic simulation studies confirmed the stability of these complexes. *In silico* analysis of CNS permeation indicated the capability of compounds in the B series, notably B3 and B4, to be across the BBB. This implies a plausible mechanism by which these designed compounds could interfere with amyloid beta aggregation, offering potential therapeutic avenues for addressing neurodegenerative conditions like Alzheimer's disease. Additionally, it is anticipated that these studies will make a significant contribution to the design and development of novel small molecules with anti-Aβ aggregation properties.

5. ACKNOWLEDGEMENT

The molecular modeling software used in this study receives support from The Scripps Research Institute and the Molecular Simulations in Drug Discovery (MSDD) Project within the Faculty of Pharmacy. This support is provided through the Mahidol University Drug Discovery and Development Platform (MU-DDD) as part of Reinventing University, Fiscal Year 2021. The author expresses gratitude to the Pharmacometrics Center at the Faculty of Pharmacy, Mahidol University, for their support in providing GastroPlusTM software version 9.8.

Conflict of interest
None to declare.

Funding
This work is supported by Mahidol University (Basic Research Fund: fiscal year 2022, grant number BRF1-034/2565).

Ethics approval
None to declare.

Article info:
Received October 2, 2023
Received in revised form November 24, 2023
Accepted December 5, 2023

Author contribution
The roles of the authors in this study were as follows: K.S. contributed to conceptualization, research design, methodology, validation, formal analysis, discussion and suggestion, writing review and editing, visualization, supervision, and project administration. S.L. and S.J. were involved in research design, methodology, investigation, formal analysis, data curation and validation, and writing-original draft preparation. Additionally, all authors have thoroughly reviewed and approved the final version of the manuscript for publication.

REFERENCES

1. Hendrie, HC. Epidemiology of dementia and Alzheimer's disease. Am J Geriat Psychiat. 1998**;**6:S19.
2. Wisniewski T, Ghiso J, Frangione B. Biology of Aβ amyloid in Alzheimer's disease. Neurobiol Dis. 1997;4(5):313-28.
3. Chen G, Xu T, Yan Y, Zhou Y, Jiang Y, Melcher K, et al. Amyloid beta: structure, biology and structure-based therapeutic development. Acta Pharmacol Sin. 2017;38:1205-35.
4. Selkoe DJ. The molecular pathology of Alzheimer's disease. Neuron. 1991;6(4):487-98.
5. Froelich-Fabre S, Bhat RV. Mechanisms of tauopathies. Drug Discov Today Dis Mech. 2004;1(4):391-98.
6. Hardy J, Selkoe DJ. The amyloid hypothesis of Alzheimer's disease: Progress and problems on the road to therapeutics. Science. 2002;297(5580):353-56.
7. Haass C. Take five-BACE and the γ-secretase quartet conduct Alzheimer's amyloid β-peptide generation. EMBO J. 2004;23 (3):483-88.
8. Lührs T, Ritter C, Adrian M, Riek-Loher D, Bohrmann B, Dőbeli H, et al. 3D structure of Alzheimer's amyloid-β (1-42) fibrils. Proc Natl Acad Sci USA. 2005;102(48):17342-7.
9. Sciarretta KL, Gordon DJ, Petkova AT, Tycko R, Meredith SC. Aβ40-Lactam(D23/K28) models a conformation highly favorable for nucleation of amyloid. Biochemistry. 2005;44(16):6003-14.
10. Sato T, Kienlen-Campard P, Ahmed M, Liu W, Li H, Elliott JI,

et al. Inhibitors of amyloid toxicity based on β-sheet packing of Aβ40 and Aβ42. Biochemistry. 2006;45(17):5503-16.
11. Petkova AT, Buntkowsky G, Dyda F, Leapman RD, Yau WM, Tycko R. Solid state NMR reveals a pH-dependent antiparallel β-Sheet registry in fibrils formed by a β-Amyloid peptide. J Mol Biol. 2004;335(1):247-60.
12. Streltsov VA, Varghese JN, Masters CL, Nuttall SD. Crystal structure of the amyloid- β p3 fragment provides a model for oligomer formation in Alzheimer's disease. J Neurosci. 2011;31(4):1419-26.
13. Johnson CN, Roland A, Upton N. New symptomatic strategies in Alzheimer's disease. Drug Discov Today Ther Strateg. 2004;1 (1):13-9.
14. Hüll M, Berger M, Heneka M, Disease-modifying therapies in Alzheimer's disease: How far have we come? Drugs. 2006;66: 2075-93.
15. Van Marum RJ. Current and future therapy in Alzheimer's disease. Fundam Clin Pharmacol. 2008;22(3):265-74.
16. Weggen S, Eriksen JL, Das P, Sagi SA, Wang R, Pietrzik CU, et al. A subset of NSAIDs lower amyloidogenic Aβ42 independently of cyclooxygenase activity. Nature. 2001;414(6860):212-6.
17. Kukar T, Golde TE. Possible mechanisms of action of NSAIDs and related compounds that modulate-secretase cleavage. Curr Top Med Chem. 2008;8:47-53.
18. Page RM, Baumann K, Tomioka M, Pe´rez-Revuelta BI, Fukumori A, Jacobsen H, et al. Generation of $A\beta_{38}$ and $A\beta_{42}$ is independently and differentially affected by familial Alzheimer disease-associated presenilin mutations and γ-secretase modulation. J Biol Chem. 2008;283(2):677-83.
19. Luo JE, Li YM. Turning the tide on Alzheimer's disease: Modulation of γ-secretase. Cell Biosci. 2022;12(2):2.
20. Du Z, Li M, Ren J, Qu X. Current strategies for modulating Aβ aggregation with multifunctional agents. Acc Chem Res. 2021; 54(9):2172-84.
21. Strohmeyer R, Kovelowski CJ, Mastroeni D, Leonard B, Grover A, Rogers J. Microglia responses to amyloid β peptide opsonization and indomethacin treatment. J Neuroinflammation. 2005;2: 18.
22. Tang M, Taghibiglou C. The Mechanisms of action of curcumin in Alzheimer's disease. J Alzheimers Dis. 2017;58(4):1003-16.
23. Ravichandran V, Sankar S, Agrawal RK. Predicting anti-HIV activity of 1,1,3-trixox [1,2,4]-thiadiazine (TTD) derivatives: 3D QSAR approach. Med Chem Res. 2009;18:511-22.
24. D'Ursi AM, Armenante MR, Guerrini R, Salvadori S, Sorrentino G, Picone D. Solution structure of amyloid β-Peptide (25-35) in different media. J Med Chem. 2004;47(17):4231-38.
25. Morris GM, Huey R, Lindstrom W, Sanner MF, Belew RK, Goodsell DS, et al. AutoDock4 and AutoDockTools4: Automated docking with selective receptor flexibility. J Comput Chem. 2009; 30(16):2785-91.
26. Morris GM, Goodsell DS, Halliday RS, Huey R, Hart WE, Belew RK, et al. Automated docking using a Lamarckian genetic algorithm and an empirical binding free energy function. J Comput Chem. 1998;19(14):1639-62.
27. Sanner MF. Python: A programming language for software integration and development. J Mol Graph Model. 1999;17(1):57-61.
28. Hudson SA, Ecroyd H, Kee TW, Carver JA. The thioflavin T fluorescence assay for amyloid fibril detection can be biased by the presence of exogenous compounds. FEBS J. 2009;276:5960-72.
29. Phillips JC, Braun R, Wang W, Gumbart J, Tajkhorshid E, Villa E, et al. Scalable molecular dynamics with NAMD. J Comput Chem. 2005;26:1781-802.
30. Vanommeslaeghe K, Hatcher E, Acharya C, Kundu S, Zhong S, Shim J, et al. CHARMM general force field: A force field for drug-like molecules compatible with the CHARMM all-atom additive biological force fields. J Comput Chem. 2009;31(4):671-90.
31. BIOVIA. BIOVIA Discovery Studio Visualizer [document on internet]. Paris: Dassault Systèmes; 2022 [cited 2023 Oct 25]. Available from: http://www.3ds.com/products/biovia/discovery-studio/visualization.
32. Kukar TL, Ladd TB, Bann MA, Fraering PC, Narlawar R, Maharvi GM, et al. Substrate-targeting γ-secretase modulators. Nature. 2008;453(7197):925-29.
33. Munter LM, Voigt P, Harmeier A, Kaden D, Gottschalk KE, Weise C, et al. GxxxG motifs within the amyloid precursor protein transmembrane sequence are critical for the etiology of Aβ42. EMBO J. 2007;26(6):1702-12.
34. Mithu VS, Sarkar B, Bhowmik D, Das AK, Chandrakesan M, Maiti S, et al. Curcumin alters the salt bridge-containing turn region in amyloid β (1-42) aggregates. J Biol Chem. 2014;289 (16):11122-31.
35. Azam F, Alabdullah NH, Ehmedat HM, Abulifa AR, Taban I, Upadhyayula S. NSAIDs as potential treatment option for preventing amyloid β toxicity in Alzheimer's disease: An investigation by docking, molecular dynamics, and DFT studies. J Biomol Struct Dyn. 2018;36(8):2099-117.
36. Laivut S, Moongkarndi P, Kitphati W, Rukthong P, Sathirakul K, Sripha K. Design, synthesis, and neuroprotective activity of phenoxyindole derivatives on antiamyloid beta (Aβ) aggregation, antiacetylcholinesterase, and antioxidant activities. Pharmaceuticals. 2023;16:355.
37. Simulation Plus. GastroPlus™ PBBM / PBPK [document on the internet]. California: Simulation Plus; 2022 [cited 2023 October 25]. Available from: https://www.simulations-plus.com/software/gastroplus.